Calculation of Vertical Parallel Wall Fires with Buoyancy-Induced Flow

H. Y. WANG, J. L. TORERO* and P. JOULAIN
Laboratoire de Combustion et de Détonique
C.N.R.S. UPR 9028 -E.N.S.M.A., Université de Poitiers
BP 109 - Site du Futuroscope
86960, Futuroscope Cedex, FRANCE

ABSTRACT

A numerical study was conducted to evaluate the use of a two-dimensional adaptation of the Discrete Ordinates Method to estimate the flame radiation energy for burning walls. The methodology extends previous work by substituting the constant soot radiative fraction, χ, approach by two-equations, a soot model and a radiative transfer equation without scattering. Predictions for the burning rate distribution, flame structure and velocity field on wall fires in a parallel configuration were carried out for one and two burning walls. The main parameter varied was the distance between the walls. Transport equations for mass, momentum, gas-phase mixture and enthalpy are solved using a finite volume method. Velocities, temperature and turbulent quantities were correlated to experimental data. A good agreement was observed between computations and experimental data. These results have implications when identifying and assessing the risk associated to the bulk storage of materials for different wall spacing/height ratio.

KEYWORDS: Vertical Parallel Wall Fire, Turbulent Burning, Buoyancy-Induced Flow

INTRODUCTION

During the last three decades, extensive information has been provided for single wall

* Present Address: Department of Fire Protection Engineering, University of Maryland, College Park, MD20742, USA

fires [1-5]. The information reported includes burning rate, flame structure and velocity fields. In contrast, the configuration where the fire occurs inside parallel walls, common to storage arrays in warehouses, has not been described by a rigorous mathematical analysis. The vertical channels between adjacent stacks offer an ideal pathway for fire growth therefore, in such circumstances, fire protection is difficult. There is a need to understand fire spread mechanisms in more detail to enable better quantification and reduced of risks by avoiding specific geometrical configurations.

Experiments [6, 7] have shown that combustion between parallel vertical walls, in which a buoyancy-induced draft develops, is more intensive than that over a single vertical wall. Unfortunately, little attention has been given so far to the description of this phenomenon. To the best knowledge of the authors, the first numerical and experimental analysis addressing wall fires in a parallel configuration is the work of Tamanini [7]. In this study a previously developed theoretical model for a single wall fire was extended to simulate a fire inside parallel walls by pre-assigning a free-parallel stream velocity. In spite of the important findings of this work, description of the characteristics of the diffusion flame and buoyancy-induced draft in the parallel configuration remained limited.

This consideration has provided the main motivation for the present work. An efficient parabolized procedure, developed recently by the authors [8], is used as the framework for this numerical study. The main advantage of the parabolized procedure lies in its rapidity and its economical storage, particularly when dealing with the strong coupling of the two initially unknown controlling parameters: the burning rate and buoyancy-induced flow. Soot and radiation models are incorporated to the numerical scheme. Predictions of the mean temperature, velocity and turbulent quantity are first compared with available experimental data [6] for a propane fire in the parallel wall configuration. Work has been undertaken to understand the effect of such geometry on the heat fluxes and the accompanying burning rate which occurs when a flame is burning between combustible surfaces.

THEORETICAL ANALYSIS

In vertical parallel wall fires, the mean cross-sectional pressure within the channel will be less than the surrounding pressure at the same elevation. The flow is solely induced and vertically accelerated by buoyant forces through the stream wise momentum equation. The basis of the mathematical model employed has been described in detail elsewhere [8] and will not be repeated here. The model incorporates the differential conservation equations of mass, momentum, energy, soot and chemical species. All symbols used in this section have their usual fluid dynamical meaning : ρ is the density, Y_i the mass fraction, u stream wise velocity, T temperature, g the gravity, r_f and r_s are the stoichiometric oxygen mass requirement for fuel and soot, respectively.

Turbulence

For the vertical parallel wall fire, the Reynolds number of the buoyancy-induced flow is usually higher than 3000, and turbulence can be considered fully developed. We have chosen to adopt the $k-\varepsilon$ turbulence model [9] because its strong and weak sides are well known. The

Reynolds stresses and fluxes are calculated through the turbulent kinetic energy, k and its dissipation, ε [9]. The fluctuating flow is also affected by the buoyancy term [10],

$$G_b = \frac{C_T C_\mu}{T} g \frac{k^3}{\varepsilon^2} \frac{\partial u}{\partial y} \frac{\partial T}{\partial y}$$

in which the normal gradient diffusion is taken into account, giving the realistic predictions for the streamlined flow. In general, the empirical constants (C_T and C_μ) are assigned the standard values [9, 10].

Combustion

The Eddy-Break-Up model [11] is used for treating the interaction between turbulence and combustion, and based on the concept of a single irreversible step reaction. The fuel reaction rate is taken to be the slowest of the turbulence dissipation rates corresponding to fuel (Y_{fu}), oxygen (Y_{ox}) or hot products (Y_{pr}), written as:

$$\dot{\omega}_{fu} = -\rho \frac{\varepsilon}{k} \min\left[C_R Y_{fu}, C_R \frac{Y_{ox}}{r_f}, C_R' \frac{Y_{pr}}{(1+r_f)} \right]$$

where C_R and C_R' are constants equal to 4 and 2 respectively.

Soot Formation and Combustion

For computational simplicity, the two-equations soot model [12], is chosen for this work to predict soot concentration (c_s). The soot formation and its oxidation are incorporated into a turbulent flow calculation in two convection-diffusion equations that compute a mean precursor particle number density and mean soot concentration. The combustion of soot particles is modeled according to the Eddy-Break-Up concept formulated as:

$$R_c = A\rho c_s \frac{\varepsilon}{k} \times \min\left[1, \frac{Y_{ox}}{c_s r_s + \rho Y_{fu} r_f} \right]$$

The activation energies, pre-exponential factors (A) and the empirical constants can be found in reference [12].

Energy

By assuming that the fluid Lewis number is close to unity, the energy equation source term is uniquely a function of the radiant flux vector. For the absorption in the flames, the gray gas assumption has so far been used and will be used here. The radiation intensity is found by solving a Radiative Transfer Equation (RTE) [13] without scattering as the soot particles are small. The RTE describing the spatial variation of radiative intensity along each direction is

solved through the use of a two-dimensional adaptation of the Discrete Ordinates Method [13]. Soot, CO_2 and H_2O are considered as the primary products, and the radiant absorption-emission properties for a non scattering gray medium, are functions of temperature and the concentration of combustion products [14].

Boundary Conditions

Three boundary conditions prescribed are: inlet, burning or inert wall and the symmetry plane. At the inlet, it is assumed here that the flow enters in the stream wise direction with a uniform axial velocity, U_0 , and at the ambient temperature and pressure.

At the wall surfaces, the non-slip condition is imposed by setting the stream wise velocity to zero. The heat flux to the burning walls due to convection, and the wall's influence on the flow, are calculated by help of the wall function method [15, 16]. For radiation, the burning wall is treated as a diffusively reflecting and emitting surface with an emissivity of 0.3. The temperature profiles along inert walls is determined using an emissivity of 1. The calculations correspond to a one-dimensional analysis of convective and radiative heat fluxes. At the symmetry plane, for the two burning walls case, the zero gradient condition is imposed.

Method of Resolution

The control volume method developed by Patankar [17] is used to discretize the partial differential equations. The mean flow equations are numerically solved by using the SIMPLEC procedure to handle the pressure-velocity coupling [18].

Of particular treatment, in the parabolized procedure, is the pressure-velocity coupling in the stream wise direction (x). The stream wise pressure gradient is assumed to be practically uniform in the cross-section (y), but strongly depend on the streamwise direction (x). The parabolized procedure starts at the inlet plane of the channel and proceeds downstream until the exit is reached. In order to start the calculation, the values of the two initially unknown parameters: the inlet velocity (U_0) and burning rate ($\dot{m}_S$), are required. This difficulty is overcame by using the parabolized technique which is described as follows.

1. A uniform distribution of the burning rate ($\dot{m}_S = 3 \times 10^{-3}$ kg/m^{2}s) is guessed for estimating the total heat release rate and a possible range of the inlet velocity (U_0) value varying from 0 to 3 m/s is prescribed according to the wall fire conditions.
2. With this inlet velocity and burning rate, the fluid flow is calculated, and the temperature values are evaluated. Convergence is achieved when the normalized residuals are less than 1×10^{-5} for each equation at each cross-section.
3. The radiation properties are specified, and the radiative source term is substituted into the energy equation which is solved to update the dynamic and thermal fields.
4. Based on these velocity and temperature fields, the burning rate is re-calculated through the convective ($\dot{q}_{conv}$) and radiative ($\dot{q}_{rad}$) fluxes.

5. This iterative procedure (2)-(4) is repeated to properly account for the non-linearity and inter linkage between the dynamic and thermal fields until the burning rate change less than 5%.
6. Finally, the inlet velocity value, U_0, of the buoyancy-induced flow is determined by the requirement that the pressure difference goes to zero at the exit. Iterative computational runs that include steps (1)-(5), have to be made to obtain a final value of the inlet velocity.

MODEL VALIDATION

In order to validate the numerical model, two experimental configurations are considered [6], as shown in Figures 1(a,b). Figure1(a) corresponds to a single burning wall case (Tests 1,3) and Figure 1(b) to the two burning walls case (Tests 2,4). Two different wall spacing, L=0.062 m (Tests 1-2) and L=0.1 m (Tests 3-4), were explored. All tests used sintered bronze burners which were located on a wall of height H = 1 m and propane as fuel. The gaseous fuel injection rate was 0.003 kg/m^{2}s, adjusted to give a theoretical heat release of 52 kW for the single burning wall case and 104 kW for the two burning walls case. Temperatures were obtained by means of fine wire analogue compensated thermocouples. Velocities and turbulent quantities were determined using a two-component Laser Doppler Velocimetry (LDV) system. All measurements for the four wall fire conditions were conducted at the height of 0.9 m. Equivalent tests with condensed fuels can not be found in the literature but are considered necessary to fully validate this approach.

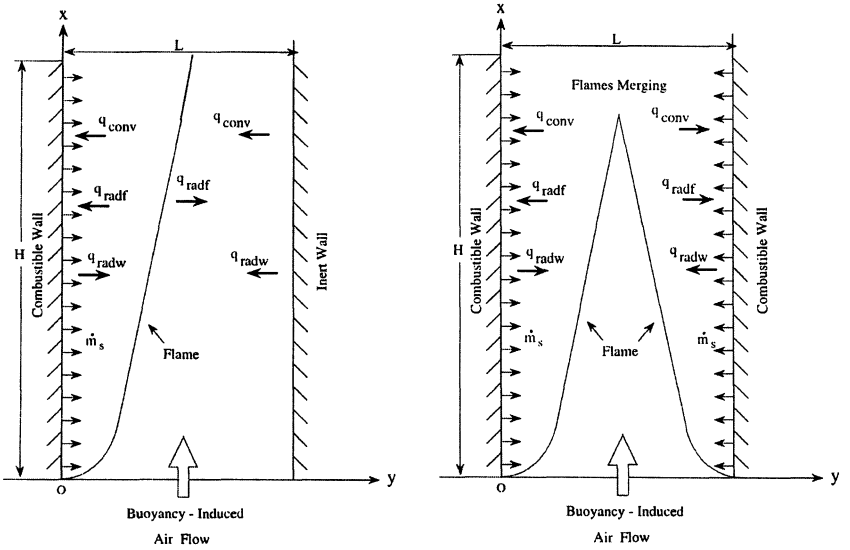

(a) Single burning wall opposed against an inert wall (b) Two opposing burning walls

Figure 1. Schematic diagram of vertical parallel wall fires with a buoyancy-induced flow

In the simulation, a higher density of grid nodes is generated using a series distribution

close to the wall. The grids used are 18 for Tests 1-2 and 24 for Test 3-4, respectively. The axial step size was selected such as it would cause the local mean velocity and temperature to change by approximately 5%. With this continuously varying step size, about 200 forward steps are required to cover the burning wall height (H) of 1 m. The integro-differential RTE is solved only in a fixed number of discrete directions using the Discrete Ordinates Method [13]. For this two-dimensional calculations 48 discrete directions spanning a full range of the total solid angle have been chosen. Global execution time on the DEC3000/alfa for obtaining the final values of the inlet velocity is about 3 hours.

Figures 2(a,b) show the comparison between the temperature calculations and the different tests. Note that the lines and symbols definition of Tests 2 and 4 in Fig.2b correspond to that of Tests 1 and 3 in Fig.2a, respectively. It can be seen that, for all cases, agreement between theory and experimental temperatures is relatively good in terms of magnitude and distribution. The temperature increases with the distance from the burning wall from about 850 K to a maximum of 1360 K, then it progressively decreases beyond the reacting zone. Calculations at different heights show a highly similar character of the temperature profiles along the burning wall. The most significant discrepancies are observed for the cases where the burning wall opposes an inert one. The model tends to underestimate temperature levels (about 150-200 K) near the inert wall as the spacing between the walls increases (Test 3, L=0.1 m) and to over estimate the location of the temperature peak as the distance decreases (Test 1, L=0.062 m).

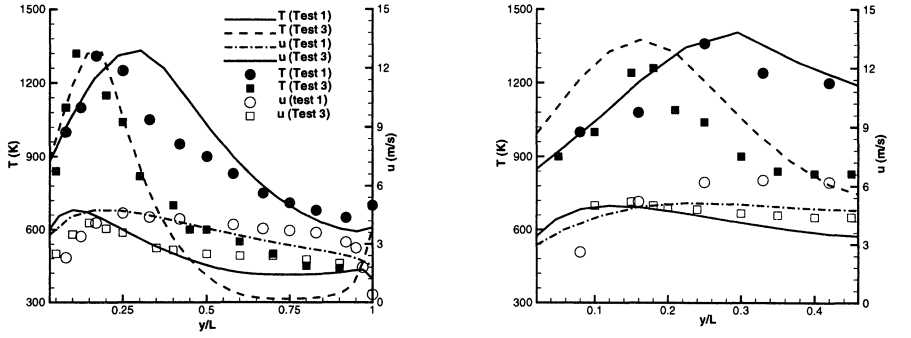

(a) Tests 1 (L=0.062 m) and 3 (L=0.1 m) Single burning wall (x/L=0.9)

(b) Tests 2 (L=0.062 m) and 4 (L=0.1 m) Two burning walls (x/L=0.9)

Figure 2. Predicted (lines) and experimental (symbols) mean temperature and velocity profiles

As shown in Figures 2(a,b), the general shape of the mean velocity profiles is correctly predicted. Agreement between prediction and experiment is relatively good except for Tests 1 and 2 for which the quantitative discrepancies appear significant with an underestimation of about 15% in the peak velocity (Test 2) and of 20% in the location of the maximum value (Test 1). Comparison between experiments and calculations for Tests 1 and 2 is difficult since buoyant instabilities are introduced as the flames approach the opposing wall or flame. The buoyant instability are not taken into account in the simulation, and this effect becomes more important as

the wall spacing decreases. Another important source of error is the actual velocity measurements. Accurate measurements of the mean velocity are usually difficult to perform as the flame fills the entire width of the gap (Test 2, L=0.062 m), inducing strong buoyant instabilities. Furthermore, a rectangular window, needed for the LDV measurements, has to be made at the height of 0.9 m on each of the burning walls introducing perturbations during the experiments.

In the vertical parallel wall fire, the flow (oxidizer) is buoyantly induced from a quiescent environment of ambient air due to thermal expansion, through the stream wise driving pressure. The inlet velocity value of the buoyancy-induced flow is determined by the requirement that the driving pressure goes to zero at the channel exit, as shown in Figure 3. In general, the driving pressure increases with the height at the lower part of the channel, attains a maximum and then decreases towards zero at the upper one. Although the case of two burning walls (Tests 2, 4) reinforces the driving pressure, the strong effect of the flame prevents air entrainment towards the channel. Consequently, when an inert wall is replaced by a burning one a decrease of the air entrainment into the channel is observed. The mass of air entrained drops from 1.3 kg/m^{2}s (Test 1) to 1.21 kg/m^{2}s (Test 2) for L/H=0.062, and from 1.43 kg/m^{2}s (Test 3) to 1.25 kg/m^{2}s (Test 4) for L/H=0.1.

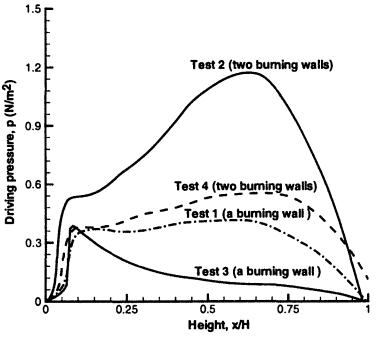

Figure 3. Prediction of stream wise driving pressure between vertical parallel burning walls for Tests 1-4

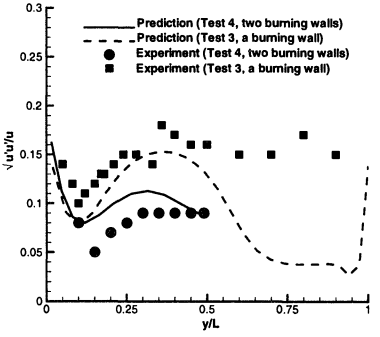

Figure 4. Predicted (lines) and experimental (symbols) profiles of the velocity fluctuation at a height of 0.9 m for Tests 3-4 (L=0.1 m)

As for the comparison for the normalized velocity fluctuations, $\sqrt{u'u'}/u$ (u is the local velocity), only Tests 3 and 4 will be compared since the results are representative of all cases studied. As shown in Figure 4, agreement between experiment and prediction is seen to be relatively good inside the reacting region. The velocity fluctuation first decreases once away from the burning wall (y/H>0.1) where turbulence is principally produced by shear stress, to a minimum at the flame sheet, and then increases in the core flow region. Moreover, the case of two burning walls (Test 4) brings about a decrease of the level of the velocity fluctuation due to re-laminarization caused by buoyancy effects. Within the cold flow region (y/L>0.5) near the

inert wall significant differences between prediction and experiments are noticeable for Test 3. The discrepancies are mainly due to three-dimensional effects [8], which may be very pronounced with the decrease of the effect of buoyancy and which are inherent to the experimental facility. It appears that, for Test 3, the discrepancies between the resulted temperature and velocity fields are associated with the underestimation of the velocity fluctuation.

RESULTS AND DISCUSSION

The model can be used to extract interesting information by considering two characteristic physical situations:

(a) When a burning wall opposes an inert wall (Fig.1a), it is important to know how the geometry affects the ease with which the surface temperature, of the inert wall, can increase beyond characteristic ignition temperatures. Pre-heating towards ignition is of great relevance since it describes the time available before involvement of remote fuels. For this work a reference value of T=600 K will be used for ignition (corresponds to typical values used for piloted ignition of PMMA in a vertical configuration). The opposing flame can be considered the pilot.

(b) Once the facing wall has ignited, it is important to understand how the geometry influences the flame structure, and as a consequence, the convective/ radiative fluxes, the accompanying burning rate and the mass of unburned fuel convected beyond the walls.

The effect of reducing the distance (L) to the burning wall (Fig.1a) on the distribution of the surface temperature of the facing inert wall is shown in Fig. 5. The wall spacing/height ratio (L/H) varies from 0.35, 0.25, 0.15, 0.1 up to 0.062. It can be seen that the surface temperature of the inert wall increases with height. Temperatures higher than 600 K are only reached as the separation (L/H) is reduced to less than 0.15. That means that once the inert wall is replaced by a PMMA one, its solid surface will pyrolyze due to heat feedback from the high temperature gases in the flame. In this work, the phenomena of the ignition and flame spread are not modeled. It is assumed that the facing inert wall (PMMA) as shown in Fig.1a, can be ignited, and once ignited, these conditions give rise to two diffusion flames as shown in Fig.1b. However, for large separation (L/H>0.2), ignition of the opposing surface does not occur and the case of a single burning wall opposed an inert one (Fig.1a) has to be considered.

Heat transfer from the flame towards the wall significantly affects the mass burning rate once the flame is established, therefore it is appropriate to conduct a systematic evaluation on the effects of confinement on convective and radiative heat transfer.

The predicted convective heat flux, $\dot{q}_{conv}$, with height of the burning wall is displayed in Figure 6. It may be intuitively expected that the effects of confinement on the fire-induced air flow and flame structure will in turn influence the convective heat transfer processes. For the high level of confinement (L/H<0.2, two burning walls case), the convection flux is found to increase at first with increase of the wall spacing/height ratio (L/H) from 0.06 to 0.1, and decrease later with further increase of that to 0.15. It is found that the highest level of confinement (L/H=0.062)

brings about a dramatic reduction in convection flux after the merging of the two diffusion flames at x/H=0.6. This is principally due to a significant flame stand-off distance induced by a lack of oxidizer at the core which in turn will reduce the temperature gradient near the burning surface. However, the moderate separation (L/H=0.1) maintains a high convective flux due to the shift of the reacting zone towards the burning surface which tends to reinforce the normal temperature gradient there. For the low level of confinement (L/H>0.1) the convective flux rapidly decreases from the highest value at the leading edge to a minimum, at the height (x/H) of 0.4, then slightly increases downstream due to the enhancement of the turbulence level. Single burning wall cases L/H=0.25 and L/H=0.35 show similar patterns than the last two burning walls case (L/H=0.15) reinforcing the notion that for low levels of confinement convection in a channel with two facing burning walls acts as two independent burning walls [3, 5]. Note also that the convective flux with the presence of an inert wall (L/H>0.2) is more important than that between two burning walls, this is due mostly to the lower turbulence level (Fig.4) in the last case.

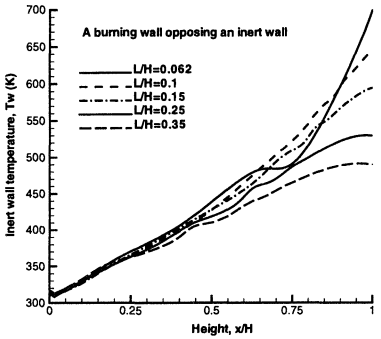

Figure 5. Evolution of the surface temperature of an inert wall as a function of wall spacing/ height ratio

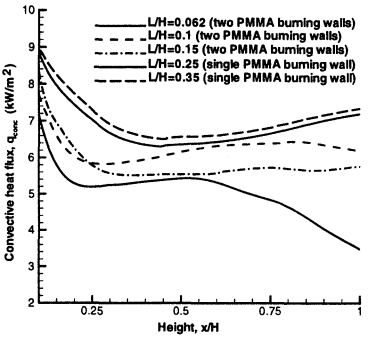

Figure 6. Prediction of the convective flux at the interface between fluid and solid burning surface as a function of wall spacing/ height ratio

Radiation flux from the high temperature gases in the flame to the burning wall, as presented in Figure 7, is computed from a discrete representation of the radiative intensity field. It can be seen that fire between two burning walls (L/H<0.2) exhibits a high radiation flux: this becomes very noticeable when the flame fills up the entire width of the gap downstream (x/H>0.6), giving direct flame impingement on both burning walls. Direct radiation from the two diffusion flames remains considerable, and the overall contribution to the heat flux from this source is higher than 80%. As the separation (L/H) increases up to 0.1, the radiative heat flux increases until it reaches a maximum. The spacing/ height ratio (L/H) of 0.1 gives the highest radiative heat flux due to the increase of radiation pathways. Further increase in L/H is found to decrease the flame radiation flux significantly (L/H=0.15) due to the attenuation of the interaction between the two diffusion flames. In the most extreme case where the ratio, L/H, varies from 0.062 to 0.1, the radiation flux is almost six times that for single burning wall case (L/H>0.2). The high contribution of the radiation flux is a consequence of the interaction of the two diffusion flames becoming very pronounced for a moderate separation (L/H<0.15).

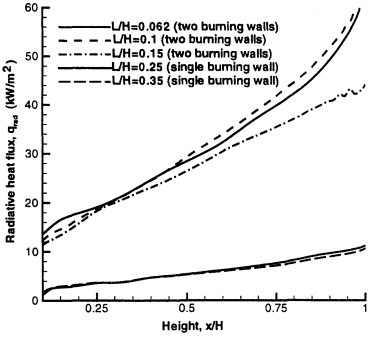

Figure 7. Contribution by flame radiation to the PMMA burning surface as a function of wall spacing/ height ratio

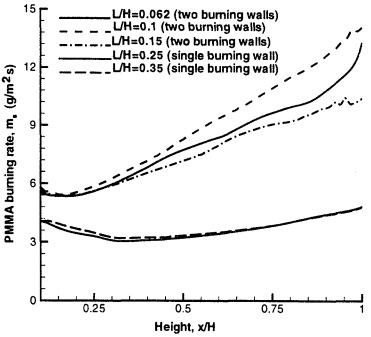

Figure 8. Evolution of the pyrolysis rate along the PMMA burning surface as a function of wall spacing/ height ratio

The PMMA burning rate, as shown in Fig.8, is controlled by the convective and radiative heat feedback from the high temperature gases in the flame to the pyrolyzing surface. It is assumed that the combustible is in equilibrium gasification, and the temperature of pyrolyzing surface of a free burning PMMA slab remains approximately constant at 636 K. The thermodynamic properties of PMMA can be found elsewhere [3, 7]. For two burning walls case (L/H<0.2), the burning rate increases with height and depend on the separation, whilst for a single burning wall case (L/H>0.2), the burning rate is independent of the separation. Changes in the burning rate are caused by a change in the dominant heat transfer mechanism from convective for single burning wall to radiative for two burning walls. Of particular interest is a maximum local burning rate occurring for a wall spacing/height ratio ($L/H \approx 0.1$).

An additional parameter of interest is the unburned fuel at the exit of the channel, since it will represent the potential flame height. The flame height can not be obtained by means of this methodology mainly due to the inherent three dimensional and elliptic nature of the flow past the channel. An evaluation of the unburned fuel will provide an estimation of the impact of the channel geometry on the flame height. Characteristic values were calculated by integrating the fuel mass fraction at the exit of the channel. In the case of a single burning wall the L/H ratio has a weak effect on the total mass of unburned fuel at the end of the channel, with this effect becoming almost negligible for L/H>0.2. The total mass flow of fuel were calculated for L/H=0.25 and gave an estimate of 2.18 x 10^{-3} kg/s, for L/H=0.35 the total mass of fuel was calculated to be 2.14 x 10^{-3} kg/s. In contrast, for two burning walls, the interaction between flames results in a significant increase in the fuel mass fraction at the outlet of the channel leading to a dramatic increase of the total mass of fuel as the distance between the walls decreases. Calculated values showed that for L/H=0.15 the mass flow of unburned fuel was 6.76 x 10^{-3} kg/s increasing to 8.6 x 10^{-3} kg/s for L/H=0.1 and to 9 x 10^{-3} kg/s for L/H=0.062.

CONCLUSION

The parabolized procedure is used to predict the thermal and dynamic fields of the vertical wall fire in parallel configuration with a buoyancy-induced flow. The separation of two parallel fuel plates has an important influence on the flame structure, and as a consequence, on the convective/ radiative heat fluxes and the accompanying burning rate.

For a large separation (L/H>0.2), a combustible material (PMMA) can not be ignited by the heat source from the opposing burning wall. In the case of a single burning wall against an inert wall, moving the inert wall away from the burning one has no influence on the radiative and convective fluxes. Thus, the burning rate along the combustible wall is only a linear function of height. However, when the separation is small (L/H<0.2), a combustible wall (ie. PMMA) can be heated by an opposing burning wall up to temperatures higher than 600 K. At this point interaction between the two burning walls occurs. Convective and radiative fluxes are more dependent on the separation of two burning walls, and as a consequence, a small change in separation can cause a significant change in burning rate. The burning rate slowly increases with a linear function of height upstream, and accelerates once the flame fills up the gap between the burning walls. The maximum increase of the burning rate is predicted at a wall spacing/height ratio ($L/H \approx 0.1$) due to the highest contribution by both convection and radiation.

The mass of unburned fuel exiting the channel increases significantly with the interaction of the two flames and is almost unaffected by the interaction between the flame and an inert wall. This has important implications on the determination of the flame height.

In spite of the above important findings, it is becoming increasingly apparent that success in assessing the hazard of combustible materials which may be used in such configurations depends on a complete modeling for the fire development. Ongoing work is considering the effect of geometry on ignition and flame spread characteristics.

REFERENCES

1. Kosdon, F. J., Williams, F. A. and Buman, C., "Combustion of Vertical Cellulosic Cylinder in Air", Twelfth Symposium (International) on Combustion, The Combustion Institute, Pittsburgh, 253-263, 1968.
2. Kennedy, L. A. and Plumb, O. A., "Prediction of Buoyancy Controlled Turbulent Wall Diffusion Flames", Sixteenth Symposium (International) on Combustion, The Combustion Institute, Pittsburgh, 1699-1707, 1977.
3. Tamanini, F., "A Numerical Model for the Protection of Radiation- Controlled Turbulent Wall Fires", Seventeenth Symposium (International) on Combustion, The Combustion Institute, Pittsburgh, 1075-1085, 1979.
4. Sibulkin, M., Kulkarni, A. K. and Annamalai, K., "Effects of Radiation on the Burning of Vertical Fuel Surfaces", Eighteenth Symposium (International) on Combustion, The Combustion Institute, Pittsburgh, 611-617, 1981.

5. Orloff, L., Modak, A. T. and Alpert, R. L., "Burning of Large-Scale Vertical Surfaces' Sixteenth Symposium (International) on Combustion, The Combustion Institute Pittsburgh, 1345-1354,1977.
6. Bellin, B., "Etude Expérimentale et Approche Numérique de l'Interaction de Deux Feu de Parois Verticales Opposées en Espace Semi-Confiné", Ph.D. Thesis, No. 28 Université de Poitiers, France, 1990.
7. Tamanini, F. and Moussa, A. M., "Experiments on the Turbulent Burning of Vertica Parallel Walls", Combust. Sci. and Tech., 23, 143-151,1980.
8. Wang, H. Y., Joulain, P. and Most J. M., "Three-Dimensional Modeling and Parametri Study of Turbulent Burning along the Walls of a Vertical Rectangular Channel' Combust. Sci. and Tech., 109, 287-307, 1995.
9. Launder, B. E. and Spalding, D. B., "Mathematical Models of Turbulence", Academi Press, London, 1972.
10. Ince, N. Z. and Launder, B. E., "On the Computation of Buoyancy-Driven Turbuler Flows in Rectangular Enclosures", Int. J. Heat and Fluid Flow, 10: 2, 110-117, 1989.
11. Cox, G. and Kumar, S., "Field Modelling of Fire in Forced Ventilated Enclosures' Combust. Sci. and Tech.,52, 7-23, 1987.
12. Magnussen, B. F. and Hjertager, B. H., "On Mathematical Modelling of Turbuler Combustion with Special Emphasis on Soot Formation and Combustion", Sixteent Symposium (International) on Combustion, The Combustion Institute, Pittsburgh, 719 729, 1977.
13. Fiveland, W. A., "Discrete Ordinates Solutions of Transport Equation for Rectangula Enclosures", Int. J. Heat Transfer, 106, 699-706, 1984.
14. Modak, A. T., "Radiation from Products of Combustion", Fire Research, 1, 339-361 1979.
15. Autret, A., Grandotto, M. and Dekeyser, I., "Finite Element Computation of a Turbuler Flow Over a Two-Dimensional Backward Facing Step", Int. J. Num. Methods in Fluids, 7 89-102, 1987.
16. Ganesan, V., Spalding, D. B. and Murthy, B. S., "Experimental and Theoretica Investigation of Flow behind an Axi-Symmetrical Baffle in a Circular Duct", J. c Institute of Fuel, 51, 144-148, 1978.
17. Patankar, S. V., "Numerical Heat Transfer and Fluid Flow", Intertext Books, Ed. M Graw Hill, New York, 1980.
18. Van Doormaal, J. P. and Raithby, G. D., "Enhancements of the SIMPLE Method fo Predicting Incompressible Fluid Flows", Numerical Heat Transfer, 147-163, 1984.